Are Liquid Metals Bulk Conductors?

Lina Sanchez-Botero, Dylan S. Shah, and Rebecca Kramer-Bottiglio*

Stretchable electronics have potential in wide-reaching applications including wearables, personal health monitoring, and soft robotics. Many recent advances in stretchable electronics leverage liquid metals, particularly eutectic gallium-indium (EGaIn). A variety of EGaIn electromechanical behaviors have been reported, ranging from bulk conductor responses to effectively strain-insensitive responses. However, numerous measurement techniques have been used throughout the literature, making it difficult to directly compare the various proposed formulations. Here, the electromechanical responses of EGaIn found in the literature is reviewed and pure EGaIn is investigated using three electrical resistance measurement techniques: four point probe, two point probe, and Wheatstone bridge. The results indicate substantial differences in measured electromechanical behavior between the three methods, which can largely be accounted for by correcting for a fixed offset corresponding to the resistances of various parts of the measurement circuits. Yet, even accounting for several of these sources of experimental error, the average relative change in resistance of EGaIn is found to be lower than that predicted by the commonly used bulk conductor assumption, referred to as Pouillet's law. Building upon recent theories proposed in the literature, possible explanations for the discrepancies are discussed. Finally, suggestions are provided on experimental design to enable reproducible and interpretable research.

1. Introduction

Room-temperature liquid metal alloys have been investigated extensively for their potential applications in stretchable electronics as electronic skin (e-skin),[1–3] stretchable conductors,[4–6] electrodes,[7,8] sensors,[2,9,10] antennas,[10] transistors,[11] energy-harvesting devices,[12–14] robots,[15–17] and flexible computational systems.[16,18–20] However, liquid metals (LM) such as eutectic gallium-indium (EGaIn) are intrinsically difficult to manipulate because of their high surface tension, giving rise to challenges in the patterning, scaling, and uniformity of EGaIn devices. Researchers have sought to improve the workability of EGaIn by embedding solid particles, such as exfoliated graphite (EIG),[21] carbon nanotubes,[22] magnetic particles,[23–26] highly crystalline Ga_2O_3,[27] copper,[1,28] silver,[29–31] and quartz.[18] The resulting

liquid–solid GaIn mixtures, or biphasic GaIn (bGaIn), can achieve a paste-like consistency without losing the electrical properties of the liquid metal. Despite this progress in workability, the electrical properties of EGaIn and bGaIn are not fully understood. Researchers have reported a wide variation of the relative change in resistance results for EGaIn (**Figure 1**a) and for composites of liquid metal[32,33] (including biphasic materials and liquid metal-embedded elastomers, or LMEEs, shown in Figure 1b). Although some samples seem to follow bulk-conductor assumptions (Pouillet's law), numerous studies show resistances below the values predicted by the model. Due to the wide range of measurement techniques used in liquid metal research, it is often unclear what differences are due to variations in intrinsic conductivity versus uncorrected errors caused by the experimental setup.

To illustrate the importance of measurement technique, consider the case of a classic two-terminal measurement system. These measurements are typically the easiest to carry out, but introduce significant measurement error.[34] In this setup, a scientist or engineer will connect a multimeter to both ends of the sample using two wires (**Figure 2**a,b). The resistance reported by the multimeter will necessarily include the resistance of the material of interest (EGaIn, bGaIn, etc.), in addition to the combined "parasitic resistance" that includes the lead wires, the contact resistance between the lead wires and the sample electrodes, and the resistance of any components (such as copper terminals, conductive epoxies, oxides,[35] etc.) between the wires and the material of interest. For higher resistance conductors (such as graphite-silicone conductive composites in sensors, which typically are in the range of several $k\Omega$[36]) the parasitic resistance is negligible. In contrast, if the sample resistance is $1\,\Omega$ compared to $0.1\,\Omega$ combined parasitic resistance (common for LM circuits), the parasitic resistance represents a fixed 10% dead-weight error.

Assuming reliable measurements can be obtained for stretchable electronics, what is the correct model for benchmarking the electromechanical behavior of liquid metal circuits? Figure 1 shows a significant range of behaviors reported in the literature, yet many authors assume that the bulk conductor assumptions (Pouillet's law[4,27,37]) are the appropriate benchmark. Typically, liquid metal samples are contained in elastomer materials that reduce their cross-sectional area when stretched, according to the material's Poisson ratio. The

L. Sanchez-Botero, D. S. Shah, R. Kramer-Bottiglio
School of Engineering & Applied Science
Yale University
New Haven, CT 06511, USA
E-mail: rebecca.kramer@yale.edu

The ORCID identification number(s) for the author(s) of this article can be found under https://doi.org/10.1002/adma.202109427.
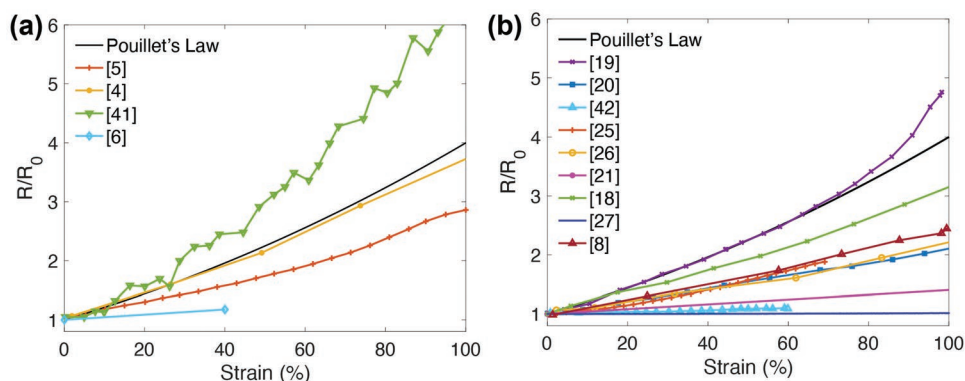
Figure 1. Compilation of reported results for relative change in resistance for a) EGaIn and b) EGaIn composites. We include biphasic GaIn (bGaIn) pastes in addition to liquid metal embedded elastomers (LMEEs), since both achieve conductivity primarily through the inclusion of liquid metal, yet the mechanics and rheology of both are different than pure eGaIn. The black, continuous line corresponds to bulk-conductor assumptions (Pouillet's law).

resulting relation between resistance change (R/R_0) and engineering strain ε (defined as $\Delta L/L$) becomes $\frac{R}{R_0} = (1+\varepsilon)^2$, which is the most commonly-used form of Pouillet's law. The relative change in resistance is conveniently a quadratic, and it is often assumed that this is the appropriate model to compare novel formulations against. However, many assumptions underlie the use of this model, which are often unaccounted for, such as: Poisson's ratio, experimental design (the parasitic resistances discussed above), sample morphology, liquid metal amount per sample, and substrate adhesion. Recent efforts have sought to model liquid metal circuits with higher fidelity, including Zolfaghari et al.'s introduction of a parameter for tortuosity in LMEEs.[37] However, as Zolfaghari pointed out, a pure liquid metal trace has a tortuosity of zero, and should therefore follow Pouillet's law. Thus, the variations observed in Figure 1a remain largely unexplained.

In this progress report, we seek to evaluate the claim that EGaIn behaves like a bulk conductor. After reviewing the experimental literature on liquid metal, we test the hypothesis that obtained resistances are strongly dependent on the testing procedure. We evaluate EGaIn traces using three conventional methods used to measure electrical resistance—four point probe (4PP), two point probe (2PP), and Wheatstone bridge (WB). Our results show substantial differences between the three measurement methods. We investigate the cause of the discrepancies, and provide empirical evidence that a significant portion of the difference between the three measurement methods can be accounted for with a single constant "parasitic resistance" which can be easily measured. However, none of our results suggest that EGaIn traces behave like a bulk conductor. Therefore, we then derive Pouillet's law from initial assumptions and discuss the advantages and limitations of this model. Seeking to determine whether biphasic liquid metal materials are significantly different than EGaIn, we then repeat the tests on samples made with a biphasic material consisting of highly crystalline Ga_2O_3 particles mixed with EGaIn. Finally, we provide a set of best practices and suggest avenues for future research on the electromechanical response of liquid metals and related materials. We hope that this discussion encourages researchers to carefully remove as many sources of experimental error as possible to improve the accuracy and

reproducibility of future research results, thereby increasing our understanding of the behaviors of stretchable electronics.

2. Electromechanical Response of Liquid Metals

Most studies that use liquid metal interconnects report resistance versus strain values significantly below that predicted by Pouillet's law (Figure 1). However, several papers also show neat EGaIn and EGaIn composites that behave similarly to bulk conductors. In this section, we review the liquid metal literature, highlighting the diversity of compositions, manufacturing methods, and measurement techniques used. We will focus on studies that report electromechanical results. For further reading, we refer readers to recent reviews on liquid metals,[38] stretchable electronics,[39] and wearable electronics.[40]

Some studies report that EGaIn behaves in agreement with Pouillet's law. For example, Zhu et al. reported stretchable conductive fibers with a triangular cross-sectional area and a core-shell structure, which consist of an EGaIn core and an elastomeric shell of Poly[styrene-b-(ethylene-co-butylene)-b-styrene] (SEBS).[4] The cross-sectional area of the fibers was tuned by varying the spinning rates: fibers with an inner diameter of ≈360 μm were obtained at a spinning rate of 1000 m min⁻¹, while larger fibers with an inner diameter of ≈670 μm were obtained at 100 m min⁻¹. A four point probe (4PP) method and a custom deformation stage were used to characterize the electromechanical properties of these conductive fibers. The larger diameter fibers only followed Pouillet's law at strain values up to $\varepsilon < 100\%$ (Figure 1a, yellow asterisks), exhibiting lower resistance change than the model from 100% to 700% strain (defined as change in length divided by initial length, or $\Delta L/L_0 = \varepsilon$). It is unclear whether the data corresponds to one sample or to the average of multiple samples, and thus it is difficult to tell how consistent these electromechanical trends are. It should be noted that Zhu et al. reported subtraction of the parasitic resistance value as part of their methodology. However, it is not immediately clear how fibers were clamped or placed in their custom deformation stage. Since liquid metal traces increase their resistance when pressure is applied,[3,41] knowledge of the clamping mechanism and parasitic resistance calculation are necessary for proper interpretation of the reported results.
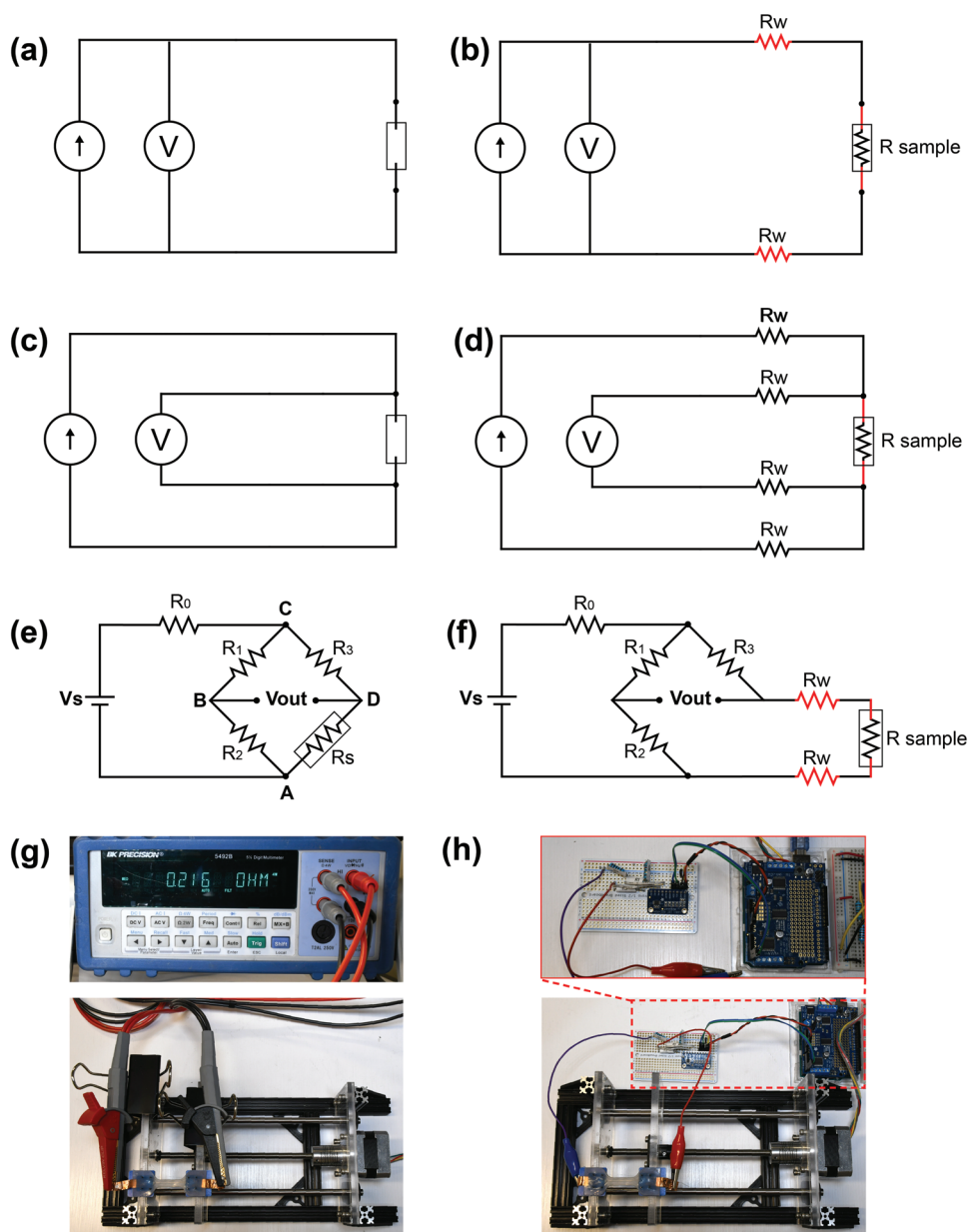
Figure 2. Summary of measurement methods used for electrical resistance measurements. Schematics are shown for a,b) two probe point (2PP) c,d) four-point probe (4PP), and e,f) Wheatstone bridge (WB). Each method indicates, in red, the unwanted "parasitic" resistances that may introduce error into the measurements of the liquid metal samples. g) Photos of the setup used for the 2PP and 4PP methods, including the multimeter (top) and tensile-testing stage (bottom). h) Photos of the WB circuit (top) and the WB circuit next to the tensile stage (bottom).

Other reports suggest that EGaIn deviates substantially from bulk conductor assumptions. Boley et al. printed traces of EGaIn onto a moving PDMS substrate.[5] The electromechanical properties of the specimens were measured with the 2PP method (digital multimeter, Fluke 87V) using a custom deformation stage. In this work, the resulting relative change in resistance follows a quadratic function with $R/R_0 \approx 3$ at 100% strain (Figure 1a, orange cross), which is 25% lower than the value predicted by Pouillet's law. During the electromechanical testing, the clamps were positioned so that the added pressure would not interfere with the liquid metal traces, and the samples were measured for five cycles. The data presented shows

five data points per measured strain; however, it is unclear if these values correspond to those five stretching cycles or to five samples. The lack of reporting prevents the assessment of reproducibility and margins of error.

By patterning serpentine or spiral microchannels filled with EGaIn, Park et al. demonstrated strain sensors that were selectively responsive to strain in particular directions (stretch along x or y direction, or pressure along the z axis).[41] Figure 1a (green triangles) shows the electromechanical response of a single channel during uniaxial strain. Using a linear approximation of Pouillet's law that is valid for small deformations ($\varepsilon < 200\%$), Park showed one sample with reasonable agreement
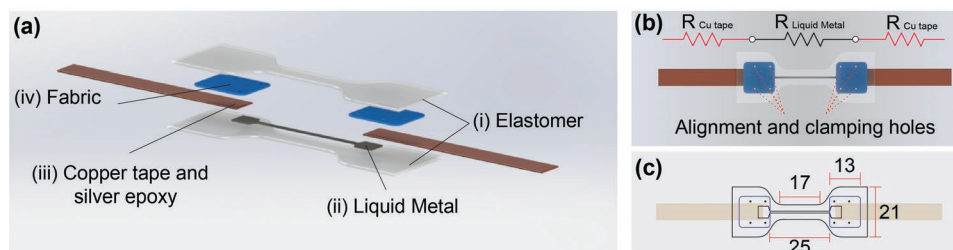
Figure 3. Schematics of the liquid metal samples. a) Exploded view of the sample components. b) Equivalent electrical circuit. c) Dimensions of the samples in mm.

between theory and experiment up to $\varepsilon = 100\%$, for a single-microchannel trace geometry (**Figure 3**a in ref. [41]). While subsequent serpentine samples were qualitatively explained to be expected to have a non-Pouillet response, the presented models did not account for the directionality of the electromechanical response (as observed in Figure 10 in ref. [41]). For these experiments, the samples were clamped in a region not containing any liquid metal, stretched using a universal testing machine (Instron 5544A), and measured using a custom 4PP resistance measuring circuit.

Gozen et al. introduced open elastomer molds with micronscale channels that were filled with EGaIn by a pressure transfer process (Figure 1a, blue diamonds).[6] The electromechanical properties of EGaIn specimens were measured to a maximum strain of 40% for a total of 50 cycles. The resistance values fluctuated within the first few cycles, followed by steady values of $R/R_0 \approx 1.18$ at 40% strain, compared to $R/R_0 \approx 2$ predicted by Pouillet's law. The axial loading was applied using a manual, lead-screw driven linear stage (Velmex UniSlide A15), and the resistance measurements were acquired with an LCR meter (B&K Precision 889B).

Similarly to neat EGaIn, some works report EGaIn composites with Pouillet-like behavior. Ozutemiz et al. presented a circuit fabrication method utilizing EGaIn's selective wetting of copper/chromium (Cu/Cr) traces.[19] In this fabrication method, the 120 nm Cu/Cr films are sputter deposited onto a PDMS substrate, then the desired circuit is patterned using a laser, followed by deposition of an EGaIn layer of several hundred μm. Although this manufacturing method uses very thin films of Cu/Cr (120nm), the contact of these elements with EGaIn may induce the formation of intermetallic compounds. The relative change in resistance of single traces was measured with a universal testing machine (Instron 5969) in conjunction with a voltage divider circuit. For this review, we extracted the data reported by Ozutemiz et al. corresponding to a sample of Cu/Cr-EGaIn embedded in PDMS and cut into a dogbone shape (ASTM D412) without HCl treatment (Figure 1b, purple x's). One of the samples exhibited good agreement with Pouillet's law in the wide range of applied strains, while the other deviated significantly from the theory, exhibiting larger values of R/R_0. In the latter example, the authors observed rupturing of the elastomer and void formation at the interface after the sample was stretched.

Yet, the majority of reported EGaIn composites suggest relative strain-insensitivity. Pan et al. sputtered thin films of Cr and Cu onto a PDMS substrate, followed by the deposition of EGaIn[20], similar to the method proposed by Ozutemiz et al.[19]

Pan reported deviation of EGaIn's electromechanical properties from Pouillet's law with $R/R_0 \approx 2$ at 100% strain (Figure 1b, blue squares), which is 50% lower than the value predicted by Pouillet's law.

Many composites made by embedding irregularly-connected droplets of EGaIn in silicone exhibit relatively strain-insensitive responses.[21,31,42–44] For example, our group recently reported one such liquid metal embedded elastomer (LMEE) that showed resistance far below Pouillet's law (Figure 1b, pink).[21] EGaIn was vigorously shear-mixed into uncured silicone to embed liquid metal microparticles into the elastomer matrix. Then, a graphite-cyclohexane suspension was added, and the composite was cast into sheets with relatively uniform thickness. After curing, the sheets could be stretched to induce microcracks and sinter the microparticles, creating a continuously-connected network of liquid metal and graphite embedded in the silicone. The electromechanical properties of the composite were measured by a custom 4PP method (a constant-current source paired with a B&K Precision multimeter) exhibiting $R/R_0 \approx 1.5$ at 100% strain.

Ford et al. demostrated a shape-morphing LMEE by embedding LM microparticles into a liquid crystal elastomer (LCE) matrix (Figure 1b, blue triangles).[42] EGaIn was shear mixed with uncured LCE to form and embed LM microparticles. During synthesis, a native gallium oxide layer formed around the LM-microparticles, requiring mechanical sintering to induce electrical conductivity. The final LM-LCE composites exhibited high electrical conductivity and high thermal conductivity. To induce reversible shape morphing, the voltage was applied to the LM-LCE composite to enable electrical joule heating and activate the shape-memory effect in the LCE. The electromechanical properties of the LM-LCE composite were measured with a USB data acquisition module (USB-6002, NI) that collected data from both the Instron 5969 materials tester and a voltage divider, exhibiting $R/R_0 \approx 1.08$ at 60% strain.

Haque et al. presented liquid metal elastomeric thin films (LET), which were made by mixing EGaIn with Styrene–Isoprene–Styrene tri-block copolymer and polybutadiene.[8] The electro-mechanical characterization of the LETs was performed by bonding them to a stretchable supporting layer (3M 4910 VHB Double-Sided Tape, 1mm thickness) and attaching copper tape electrodes. LETs were mechanically stretched in an Instron 5944 mechanical testing machine, and resistance was measured using a Keithley 2460 source meter with capability for 2PP and 4PP modes. The resulting relative change in resistance at 100% strain was reported to be ≈ 2.5, lower than the value predicted by Pouillet's law.

Pastes containing liquid EGaIn with solid filler particles, or what we will refer to as biphasic GaIn (bGaIn), have also become a field of active research, as several biphasic materials have been reported to be strain-insensitive. A liquid metal paste consisting of EGaIn and SiO_2 (quartz) particles was prepared by Chang et al. The SiO_2 particles were dispersed in the EGaIn using a ball-milling method, creating a paste with excellent electrical and rheological properties. The electromechanical properties of the material were tested on traces of the paste painted onto spandex fabric substrates. Data was gathered with an acquisition unit (34972A, Agilent) with capability for 2PP and 4PP acquisition modes. The sample exhibited a relative change in resistance similar to the theoretical value at smaller strains ($\varepsilon < 20\%$), but then deviated to lower values resulting in $R/R_0 \approx 3.1$ at $\varepsilon = 100\%$.[18]

Several research groups used nickel particles as their filler material. For example, Guo et al. manually mixed nickel microparticles with EGaIn at different concentration ratios that resulted in a Ni-GaIn amalgam (Ni-GaIn) paste[25]. The Ni-GaIn paste was printed on an Ecoflex substrate directly by a rolling brush. Flexible coils with a diameter of 4 cm were prepared, and their relative change in resistance during stretching was ≈1.9 at 70% strain (Figure 1b, orange cross). The resistance measurement method was not disclosed. Daalkhaijav et al. sonicated nickel particles into EGaIn, reporting $R/R_0 \approx 2$ at 100% using a 4PP measurement technique (Figure 1b, red circles).[26] By varying the nickel content, the size of nickel particles, and the sonication energy, different rheological properties could be obtained, although it is unclear how these process parameters would affect the electromechanical properties of the biphasic material.

In our previous work, motivated by the assumption that neat EGaIn is a bulk conductor, we developed a biphasic gallium indium (bGaIn) material to explore its electromechanical properties. To obtain this new bGaIn, EGaIn was sonicated in ethanol, spray-printed onto silicon wafers, and then baked at 900 °C to promote the in-situ formation of β-Ga_2O_3 (Figure 1b, blue line).[27] After this, the biphasic mixture was transferred to different substrates, such as PDMS and VHB (VHB 4905, 3M), utilizing various methods, including transfer-printing and manual scraping. Using a Wheatstone bridge to measure the resistance of rectangular traces, relatively strain-insensitive behavior of the samples was observed ($R/R_0 \approx 1.06$ at 100% strain on PDMS). Nevertheless, more detailed study of the samples revealed that our own results varied with measurement method, exhibiting higher relative change in resistance when 2PP and 4PP were used. This finding motivated us to compile the present progress report.

The presented literature review raises the question: What is the true electromechanical behavior of EGaIn? The wide range of measurement techniques, experimental parameters and lack of cross-validation between studies have made it difficult to interpret the strain (in)sensitivity observed in EGaIn samples, which should behave identically across studies, since EGaIn is a specific mixture of gallium and indium. As novel formulations of bGaIn and EGaIn composites emerge with the claim of strain-insensitivity, to what degree are these materials truly strain-insensitive, and when is their behavior similar to previously reported materials? When working with low-resistance

conductors, it is crucial to carefully report and ideally standardize the techniques used for sample preparation and resistance measurement, to ensure a fair comparison with prior art. In the following sections, we scrutinize some of the most commonly used techniques for resistance measurement, before returning to a deeper discussion of the relevant theory and other experimental design considerations.

3. The Importance of Measurement Technique

In this study, we investigate three commonly-used measurement methods found in the stretchable-electronics literature: two-point probe (2PP),[5] four-point probe (4PP)[4,41] and Wheatstone bridge (WB)[27] (Figure 2).[34] In brief, the 2PP method is equivalent to the common multimeter setups used in many research, educational, and home settings. The WB method can have relatively high sensitivity, and is well understood. Both 2PP and WB methods are simple to implement, but relatively error-prone. To reduce errors when measuring low resistance specimens, some researchers use a 4PP method.

The 2PP method consists of two electrodes, one at either end of the sample (Figure 2a). The resistance is measured by supplying the circuit with a constant current source and measuring the voltage across the sample with the same probes. Consequently, the measured voltage is across both the sample (R_s) and resistance of the leads (R_w) (Figure 2b). If the values of the two lead wire resistances are of the same order of magnitude as the specimen ($R_w \approx R_s$), the reported resistance value will be inaccurate.

The effects of the resistance from lead wires may be avoided by using the four-point probe method (Figure 2c,d). In a 4PP measurement, the current source circuit and the voltage sensing circuit are separated. If the input impedance of the voltage sensing circuit is sufficiently high, then the current flowing through R_w is minimal. This means the voltage drop across R_w can be neglected, and finally, the voltage sensing circuit only measures the resistance across the sample, as desired (Figure 2d). In other words, the resistance of the lead wires (R_w) is ignored, and the reading is solely dependent on the sample's resistance (R_s). The 4PP method produces relatively accurate measurements of samples with low resistance values. However, the 4PP method is not recommended for samples with high resistance values, since the assumption of zero current flowing through the voltage-sensing circuit's lead wires may become invalid.

A Wheatstone bridge is another conventional method to measure static or dynamic electrical resistance (Figure 2e). Here, we utilize a Wheatstone bridge with three fixed resistors and one variable resistor (R_s, our samples). In a Wheatstone bridge, a voltage V_s is applied between points A and C, and each half of the bridge (R_1, R_2 and R_3, R_s) forms a voltage divider. If the voltage measured between points B and D (V_{out}) is zero, the bridge is balanced; conversely, the bridge will be unbalanced when a $V_{out} \neq 0$. Any change in the sample resistance (R_s) due to tensile deformation will unbalance the bridge, making it suitable for the measurement of dynamic electrical resistance. It should be noted that our Wheatstone bridge shown in Figure 2f has an additional resistor R_0 that was used to limit the current

flowing through circuit. The derivation of the equation used in the calculation of the resistance value for the liquid metal samples can be found in Supporting Information.

Similar to the 2PP method, lead wire resistance has a significant impact on the operation of the circuit (Figure 2f, indicated by the red R_w resistors). The error is negligible if $R_w \ll R_s$, but if $R_w \gtrsim R_s$, this source of error can result in significant signal degradation. For example, our two alligator leads have a total resistance of 0.85 Ω as measured using the 4PP method, compared to sample resistances of the order of 0.5 Ω.

To illustrate the differences in the measurements methods, we manufactured our samples with a dogbone-shaped design filled with a rectangular conductive trace with two square end electrodes (**Figure 3**). Dogbone designs have been shown to be reliable and mechanically robust in other literature. Indeed, the ASTM standard for testing rubber in tension (ASTM D412) suggests using a dogbone design, and utilizing the gauge length (17 mm in our samples) as the unstretched length for strain calculation ($\Delta L/L_0 = \varepsilon$). Samples were made by depositing EGaIn onto Dragon Skin 10 (Smooth-On, Inc.) silicone films while using a polyethylene terepthalate (PET) mask. To interface the liquid metal to the measurement circuits, copper tape was attached to the ends of the sample using silver epoxy. The interfaces were then reinforced with fabric squares to prevent stretching at the interfaces. Finally, the specimens were encapsulated with another layer of Dragon Skin 10 and cut into a dog-bone shape using a CO_2 laser (ULS 3.0, Universal Laser) (Figure 3a). The electrical resistance of liquid metal samples tends to increase with increasing applied pressure, due to the

reduced cross-sectional area of the samples under mechanical compression. To avoid mechanical compression during tensile testing, four holes were also laser cut into the interface fabric area, to align and secure the samples to the tensile stage (Figure 3c). The EGaIn sample had a semi-circular cross-section, as seen in the micro-computed tomography (microCT) images shown in Figure S2a,b, Supporting Information.

We manufactured EGaIn samples, and characterized their electromechanical response using the three methods (**Figure 4**). The measurements for 2PP and 4PP methods were acquired using a digital multimeter (B&K Precision model 5492B), interfaced with a set of kelvin probes (Pomona electronics, model 6730) as test leads (Figure 2g). The Kelvin test leads have a resistance of 0.1 Ω, as measured by connecting the clips to each other and using the 2PP method. We note that the contact resistance between the test leads and the electrodes of some setups may be non-negligible. However, we found the resistance to vary negligibly, within measurement precision (≈0.001 Ω), with different orientations and contact areas between the leads and electrodes.

Five specimens were tested to get a mean value of the material behavior. The EGaIn samples have a characteristic resistance value of about 0.2 Ω, including 0.1 Ω from the electrode materials. All dynamic electrical resistance measurements were made with a custom tensile stage controlled using an Arduino Uno (Arduino, AG) (Figure 2g,h).

Across all specimens and measurement methods, we observed that the electrical resistance monotonically increased with increasing strain. The primary reason for this behavior is
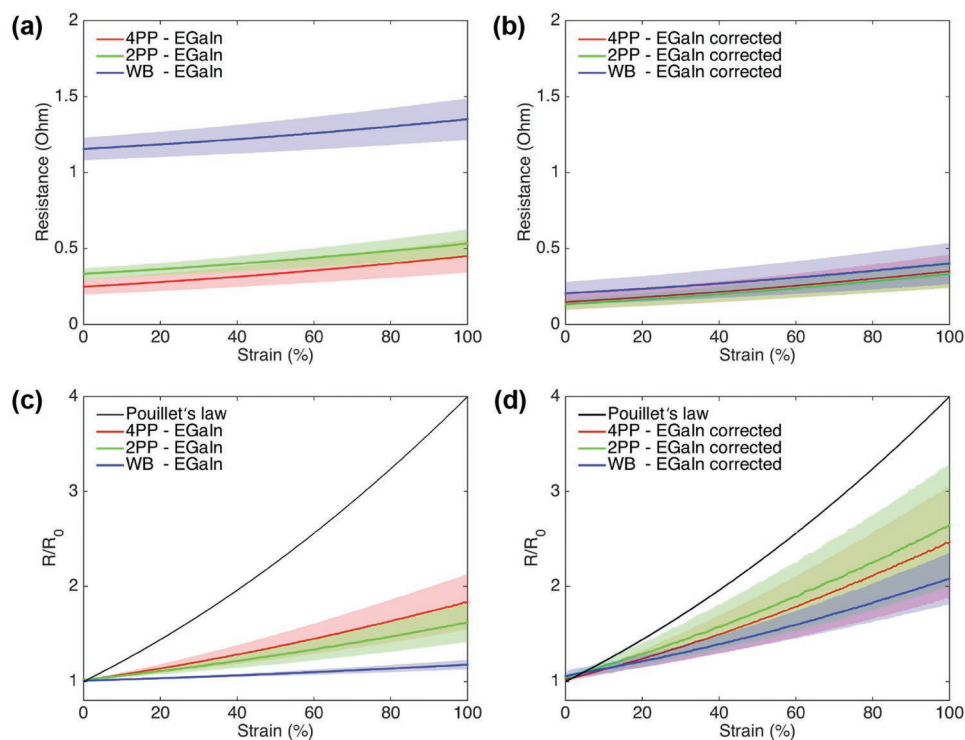

Figure 4. Electromechanical behavior of EGaIn. a) Resistance responses of the dogbone shaped samples under a tensile strain up to $\varepsilon = 100\%$ with the three electrical resistance measurement methods and their corresponding b) corrected resistance data. c) Relative change in resistance R/R_0 of EGaIn under a tensile strain up to $\varepsilon = 100\%$ and d) corrected R/R_0 data. The shaded areas represent one standard deviation for five samples.

**ADVANCED
SCIENCE NEWS**

www.advancedsciencenews.com

**ADVANCED
MATERIALS**

www.advmat.de

that, during elongation, the channels increased in length and decreased in cross-sectional area. However, additional factors are likely at play, as discussed later in this manuscript.

Although a similar rate of change is observed in the resistance of EGaIn using the three measurement methods, (Figure 4a), the magnitude of the reported resistance differs between methods. For example, the average initial resistance estimated for EGaIn with the 4PP method is 0.25 Ω, while the 2PP and WB methods yielded 0.33 and 1.15 Ω, respectively (Figure 4a). One important observation is that the 4PP and 2PP methods yielded different initial resistances for EGaIn, despite the fact that 4PP and 2PP used the exact same experimental setup (Figure 2). As mentioned above, the 2PP test lead resistance value is 0.1 Ω, which is 40% of the average value of the EGaIn samples. Larger parasitic resistances will result in a larger difference between 2PP and 4PP techniques. Put another way, the 2PP technique is more susceptible to experimental errors introduced by the connection between the measurement device and the sample. A similar discrepancy can be observed for the WB method: the estimation of the initial average resistance value using WB is ≈4.6 times larger than the value obtained with 4PP for EGaIn, owing to the relatively high resistance values of the alligator clips (0.85 Ω) used in this configuration.

The resistance of the electrode materials (copper tape and silver epoxy) was also estimated using the 4PP method. Both electrodes have a total resistance value of 0.1 Ω, which is as high as the test lead resistance of the 2PP method. Using this information in consultation with the electrical diagrams of Figure 2, the estimated resistance values for the samples with each method were then corrected by subtracting the extra resistance values (Figure 4b). Specifically, data acquired with the 4PP method was corrected for the electrodes' resistance, while the 2PP and WB methods were corrected for test lead wires and electrode resistances. The resulting curves for 4PP and 2PP methods overlap, with average initial resistances values of 0.15 and 0.14 Ω, respectively.

These results highlight the importance of understanding the assumptions behind the measurement methods used in an experiment. For example, sample electrode resistances should be considered when performing 4PP resistance measurements, and in some cases it would make sense to adjust the data prior to publication and clearly report the correction factors used. In addition, the corrected data acquired by the WB method are higher than 2PP and 4PP methods at lower strain, but the difference between measurement techniques decreases at higher strains. The initial average resistance for EGaIn, after correction, is estimated by the WB method to be 0.2 Ω. Although this value is not significantly higher than those obtained with the corrected data for 4PP and 2PP, the overlap is not perfect, implying that unaccounted resistance from other parts of the circuit configuration may still be affecting the data.

3.1. Pouillet's Law

Typically, liquid metal samples are contained in homogeneous elastomers that reduce their cross-sectional area during stretch. It has been widely accepted that the relation between resistance change and mechanical strain for liquid metal samples follows

Pouillet's law,[4,27,37] which describes the resistance of an ideal homogeneous conductor with a uniform cross section as a function of its resistivity and dimensions:

$$R = \rho \frac{L}{A} \tag{1}$$

where R is the sample's resistance, L is the length, A is the cross-sectional area of the sample, and ρ is the resistivity of the material. The resistivity ρ is the reciprocal of electrical conductivity σ, and for EGaIn $\sigma = 3.4 \times 10^6$ S m^{-1} at 22 °C.[38,45,46] If changes in length and cross-sectional area are denoted by ΔL and ΔA respectively, the resulting relative resistance change of the samples becomes

$$\frac{R}{R_0} = (1+\varepsilon)^{1+2\nu} \tag{2}$$

Hence, a nonlinear relation between resistance response and strain is predicted, where ν is the Poisson's ratio. Incompressible materials, such as Sylgard 184 (commonly referred to in the literature as simply PDMS), exhibit a Poisson's ratio of 0.5. Most authors take the incompressibility assumption for liquid metal materials, yielding the relation between resistance change and engineering strain (defined as $\Delta L/L$)

$$\frac{R}{R_0} = (1+\varepsilon)^2 \tag{3}$$

where R_0 is the unstretched resistance. Finally, we have arrived at the form of Pouillet's law that has seen widespread use in the stretchable electronics field and beyond.[4,27,37] Complete derivation of Equation (3) can be found in Supporting Information.

To test the validity of Pouillet's law on our samples, we can simply divide the resistance measurements by each sample's initial resistance (Figure 4c). The response of the EGaIn samples measured with 4PP and 2PP was nonlinear and gradually increased with strain, with a higher change in resistance for the 4PP curve. On average, R/R_0 increased to 1.83 when $\varepsilon = 100\%$ for 4PP method, and 1.62 for 2PP method. This is expected, since the 4PP method has a smaller parasitic resistance. Conversely, the EGaIn samples measured with WB method exhibited an almost strain-insensitive resistance response, indicating a maximum R/R_0 value of 1.17 at 100% strain. While all measurement methods reported the same absolute changes in resistance (Figure 4c), the relatively high parasitic resistance in the WB circuit results in lower relative changes in resistance (Figure 4c).

Applying the previous corrections to the data (Figure 4d), we again see a better agreement between the three measurement methods. However, although the WB data overlaps with the corrected results for 4PP and 2PP methods, an underestimation is still apparent after correction. In addition, a higher nonlinear R/R_0 response was observed for all three methods.

Although these results fit within the ranges published for EGaIn samples (c.f. Figure 1), none of our recorded data—raw or corrected—closely follows the trend predicted by Pouillet's law. This suggests that other factors (such as cross sectional geometry, trace shape and regularity, and quantity of encapsulated liquid metal) may also affect the electromechanical behavior of EGaIn samples, resulting in significant deviations from the predicted Pouillet's law (Equation (3)).

**ADVANCED
SCIENCE NEWS**

www.advancedsciencenews.com

**ADVANCED
MATERIALS**

www.advmat.de

Other authors have proposed several mechanisms for non-Pouillet behavior. For example, Zhu et al.[4] reported different responses of the relative change in resistance R/R_0 for two types of ultra stretchable fibers filled with EGaIn (as mentioned previously in the section "Electromechanical Response of Liquid Metals"). The EGaIn core of both fibers had a triangular cross-section, but their nominal diameter was different. The narrower fibers showed a similar change in resistance as that predicted with Pouillet's law. In contrast, the fibers with a larger diameter exhibited lower changes in resistance during deformation, and tended to change their cross section from triangular to a circular shape as the fibers were stretched. The authors generated theoretical curves for both cases; the triangular cross-section model matches Pouillet's law, while the triangle-to-circle cross section model has a lower R/R_0 response at high strain levels. However, the equations used were not explicitly stated, so we were unable to independently evaluate the model.

In another work, Neuman et al.[47] used spray deposition of liquid metal onto silicone substrates and reported resistance values as a function of trace length and trace width. They observed that thinner traces exhibited higher resistance values than thicker traces. However, by plotting the resistance as a function of trace length divided by cross-sectional area, the estimation of the EGaIn resistivity using Pouillet's law (Equation (1)) was within 10% of the value reported in the literature, suggesting that Pouillet's law is accurate at zero strain (unstretched). In the same work, different geometrical patterns of liquid metal samples (serpentine, spiral, etc.) exhibited different responses to strain. However, the authors did not provide an analytical solution to predict response a priori, leaving many questions unanswered.

Seeking to explain recent non-Pouillet behavior observed across several studies on LMEE, Zolfaghari et al. presented an FEM-informed theory that could generate curves similar to those found in the literature.[37] Zolfaghari suggested that the tortuosity of the connected liquid metal bubbles dictated the electromechanical properties of the final composite.[37] Specifically, FEM simulations showed that the electromechanical properties are influenced by LM droplet spacing and the shape of the connected conductive pathway.

In a similar vein of thought, it has been suggested that specific morphologies and substrates may induce lower changes in the electromechanical response of liquid metal samples. Ma et al.[48] fabricated a liquid metal fiber mat that exhibited an R/R_0 of 1.4 after 100 cycles at $\varepsilon = 1800\%$. The stretchability and electrical stability were ascribed to the wrinkled structures formed by the relaxation of prestretched substrates. Wrinkled structures tended to dissipate the induced strain during large deformations. Similarly, Park et al.[49] developed a deformable hydrogel with an R/R_0 of 2.3 at a strain value of 1500%. In this case, the resistance response was ascribed to the hydrogen bond interaction between the naturally formed gallium oxide in EGaIn and the hydroxyl groups of their substrate. They also showed that the resistance of different loadings of EGaIn responded differently under deformation, with the lowest EGaIn loading showing a higher change in resistance.

In sum, our experimental results did not match the bulk-conductor model (Pouillet's law), yet we cannot definitively state

which experimental procedures or fabrication steps have lead other authors to find bulk-conductor behavior on EGaIn traces. Correcting for the parasitic resistance led to higher R/R_0 values, yet there were still significant gaps between our trendlines and Pouillet's law (Figure 4d). Several explanations have been proposed in the literature, including the importance of trace geometry and the tortuosity of the conductive paths through traces, in addition to the presence of nonuniform cross-sectional shapes. However, to definitively provide a theoretical model to explain the totality of reported literature, we still need additional studies pairing theory with controlled experiments to isolate the marginal contribution of each of these proposed contributors to the final system-level electromechanical behavior.

4. Measurements on bGaIn

Reflecting on what we have learned through this study, we raise the question: does the introduction of solid particles, to make bGaIn, dramatically change the importance of measurement method and interfacing on resistance measurements? As seen in Figure 1b, numerous previous studies on different bGaIn formulations suggest that bGaIn is uniformly non-Pouillet. For example, in our previous paper, we reported measurements using a Wheatstone bridge, and found that our bGaIn was far less resistive than the predictions from Pouillet's law.[27] Here, we use our bGaIn formulation as a case study on the influence of solid particles on the conclusions derived above regarding EGaIn (namely, that 4PP measurement technique reduces error, and that there are still significant differences between measurements and Pouillet's law). While other biphasic formulations could, in principle, behave quite differently from ours, this set of measurements should serve as a cautionary, representative tale and point of reference for other researchers.

We made five bGaIn specimens, finding remarkably similar conclusions as we drew from the EGaIn samples. For example, the bGaIn samples had an average initial resistance of 0.4 Ω for bGaIn (including ≈0.1 Ω electrode resistance), which was larger than EGaIn (0.25 Ω, including ≈0.1 Ω electrode resistance). The resistance of bGaIn samples as reported by 2PP is higher (0.49 Ω), and WB is still higher (1.41 Ω, or 3.6 times the 4PP value of 0.4), following a similar trend as the EGaIn samples (**Figure 5**a,c). For 4PP and 2PP methods, a nonlinear response is observed, with average R/R_0 values at 100% strain of 1.72 and 1.61 respectively. In contrast, the WB method yielded a relatively strain-insensitive response, with an average R/R_0 value of 1.24 at 100% strain. The electrode resistance was also 0.1 Ω for bGaIn samples, representing 30% of the average value of the bGaIn samples. Using the same correction process used for EGaIn to correct the bGaIn data, we see reasonable overlap of the curves for 4PP and 2PP methods, with average initial resistances values of 0.3 and 0.29 Ω, respectively (Figure 5b,d).

These findings suggest that the introduction of solid particles may change the electromechanical behavior, but biphasic mixtures do not eliminate the need to account for electrode resistance and use a suitable measurement technique (namely, a 4PP method). Further, comparing Figures 4c and 5c, we note that EGaIn and bGaIn initially appear equally "strain-insensitive."
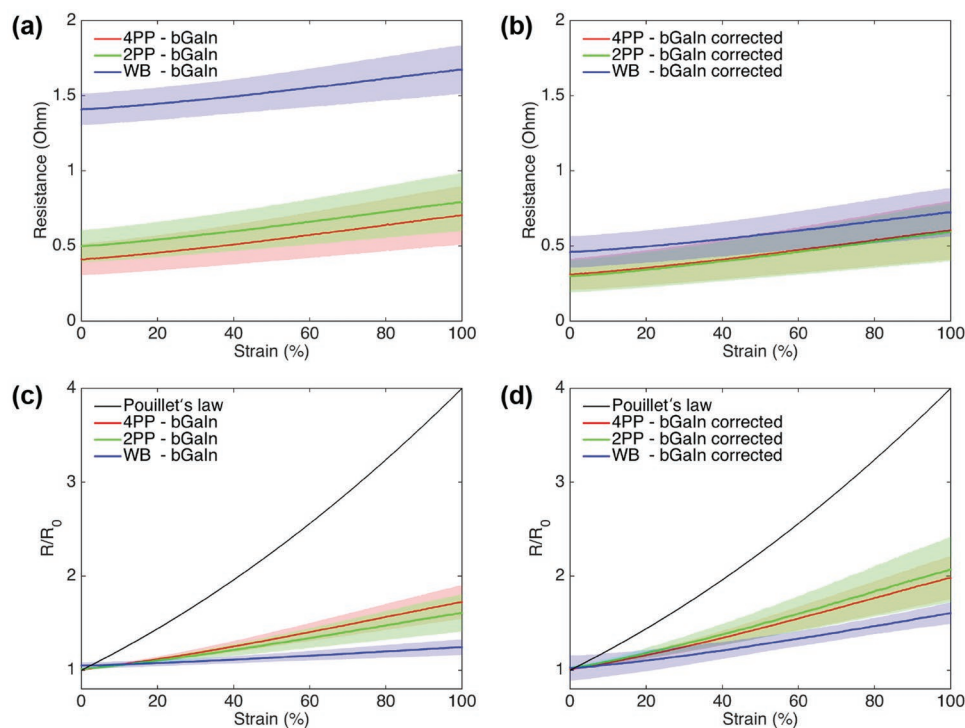
**ADVANCED
SCIENCE NEWS**

www.advancedsciencenews.com

**ADVANCED
MATERIALS**

www.advmat.de

Figure 5. Electromechanical behavior of bGaIn. a) Resistance responses of the dogbone shaped samples under a tensile strain up to $\varepsilon = 100\%$ with the three electrical resistance measurement methods and their corresponding b) corrected resistance data. c) Relative change in resistance R/R_0 of bGaIn under a tensile strain up to $\varepsilon = 100\%$ and d) corrected R/R_0 data. The shaded areas represent one standard deviation for five samples.

However, after correcting the data to remove parasitic resistance caused by the different measurement techniques, we see that bGaIn appears slightly more strain insensitive (comparing Figures 4d and 5d).

5. Outlook

In summary, we have thoroughly examined the literature, and conducted experiments, to shed light on a central question: are liquid metals bulk conductors? We found countervailing evidence, therefore failing to reject the null hypothesis. In our investigation of Pouillet's law, we found several factors that may contribute to the electromechanical behavior of EGaIn, but further study is needed to synthesize all of the hypotheses into a coherent theory. Additionally, in the course of this investigation, we uncovered several tips that should help standardize the reporting of the electromechanical response of stretchable circuits.

For example, we showed that when measuring low-resistance materials, the resistance of the test lead wires can introduce significant error if a 2PP or WB measurement method are used, suggesting the need for using a four-point probe method. Furthermore, additional errors can be introduced if there is significant contact resistance at the interfaces between the sample and its electrodes (often copper strips), and if the sample design includes significant portions of liquid metal that are not stretched during sample elongation. The 4PP method could be carried out using four independent copper wires connecting to the traces (two on each side), eliminating the copper from

the measurement. Independent measurements of these other "parasitic resistances" can be carried out and used to reduce—but not fully eliminate—the measurement error. Despite these subtle experimental complexities, we emphasize that simply using a four-point probe method will eliminate much experimental error and should generally be preferred over 2PP or WB techniques.

Determining the relative effect of each influential factor on the samples' electromechanical response requires standardized data and reproducible reporting. While we recommend using the 4PP method and correcting for electrode resistance whenever possible, not all labs have access to a reliable 4PP measurement system. Hence, transparently reporting which method was used as well as all (if any) corrections applied is essential. Additionally, experiments with a perfect measurement system will still have errors introduced during manufacturing, making it important for researchers to report values obtained using multiple samples and report a measure of variation, such as standard deviation or confidence intervals. Such reporting will allow each result to be evaluated objectively, with appropriate validations and reproductions carried out by other independent researchers. Finally, we note the lack of standardized practices to characterize stretchable electronics, despite the potential sensitivity of measurements on numerous other experimental procedures. For example, Park et al.[41] presented liquid metal devices that exhibited change in electrical resistance under both extension and compression. This result implies that the position of the clamps used in the electromechanical characterization may also affect the resistance values of liquid metal samples.

Utilizing 4PP and standardized testing methods, we have a few suggested experiments for future work investigating the electromechanical behavior of liquid metal circuits. However, this list is by no means exhaustive, and we merely suggest these experiments as examples. First, to investigate the effect of cross-sectional geometry, samples could be manufactured with intentional variations in cross-section, such as traces with constant circular cross-section versus traces with thinner and thicker sections, where injection methods may enable more precise control over cross-section. Additionally, comparing the different designs' electromechanical response with their cross-sections (rigorously quantified using, for example, micro computerized tomography imaging) could yield conclusions about the effect of trace uniformity. Other experiments could test whether the clamped end-regions effect the samples' electromechanical response, for instance by varying the end-regions' volume. Larger volumes could flow into the main trace area and prevent reductions in the cross-sectional area, thereby reducing the relative resistance change. To measure the effect of Poisson's ratio on the electromechanical response, samples could be made in different substrates and observed optically during stretch, yielding instantaneous Poisson's ratios for the stretching curve. While authors typically assume a constant Poisson's ratio, such as 0.5, we have found that silicones, such as Dragon Skin, can have nonconstant Poisson's ratio.[50] An interesting open problem complicating all of these proposed studies is how to unify the theory for the electromechanical response of pure EGaIn traces, LMEEs, and bGaIn. For example, should bGaIn be modeled more like EGaIn, or as a tortuous LMEE-like conductive network? Does the introduction of solid particles induce sufficient oxide and microstructuring to make bGaIn behave more like a tortuous path in an LMEE?

We hope these considerations can serve as a point of reference for future standardization efforts, thereby improving the inter-study comparability and furthering the theory and understanding of liquid metal circuits. By carrying out controlled studies on the effects of different variables, such as sample geometry, cross-sectional uniformity, and sample preparation techniques, we hope that future advances can yield more reliable and predictable stretchable electronics for healthcare, soft robotics, and wearable electronics.

6. Experimental Section

Sample Preparation: Gallium (Ga, 99.99%) and indium (In, 99.99%) were purchased from Rotometals, USA. Ethanol (200 proof) was obtained from VWR. Silicon wafers were obtained from UniversityWafer, Inc (75 mm diameter, boron-doped, <100> orientation, polished one side). Dragon Skin 10, parts A and B were purchased from Smooth-On.

Eutectic gallium-indium (EGaIn) alloy was prepared by mixing 75.5 wt% Ga and 24.5 wt% In and heating at 200 °C on a hot plate overnight. Biphasic gallium-indium (bGaIn) was prepared using a three step process (similar to the procedure proposed by Liu et al.[27]): (1) EGaIn nanoparticles (EGaIn NPs) suspension preparation, (2) Spray-casting of EGaIn NPs onto silicon wafers and (3) Thermal sintering process. The EGaIn NPs suspension was prepared by weighing 1.8 g of EGaIn into a 5 dram vial (Kimble) using a 3mL syringe with a 20-gauge needle. Then, Ethanol (11 mL) was slowly added, followed by sonication using a probe sonicator (Qsonica, Q700) coupled with a 1/4 inch diameter microtip (part number 4420) at 30% amplitude for 2 h. During the sonication process, the sample temperature was controlled by a water bath (Cole–Parmer Polystat) kept at 6 °C. The EGaIn NPs suspension was then poured into a 50 mL falcon tube and 5 mL of ethanol were further added.

Thin films of EGaIn NPs were prepared by spray-casting the solution of EGaIn NPs onto four silicon wafers using a customized 3D printer (Monoprice Maker Select v2). The solution was spray-printed at a constant rate (0.3 mL min^{-1}) using compressed air (20psi) blown over a 20-gauge stainless steel needle. The *x*, *y* positions were determined to cover the area of the four silicon wafers following a serpentine pattern, with the *z* height set so there was a 55 mm gap between the syringe needle and the printer bed. The printing bed speed was set to 5 mm s^{-1}. The weight of the film after five coatings was ≈180 mg for each silicon wafer. The resulting films were thermally treated at 900 °C for 30 min. bGaIn powder was obtained after the films were scraped from the silicon wafers with a razor blade, transferred to a vial, and shaken vigorously using a vortex mixer. The bGaIn powder was then mixed with EGaIn at a solid concentration of 50 wt%.

Electromechanical Characterization: The specimens were fabricated with the dimensions presented in Figure 3. First, a film of Dragon Skin 10 (DS10) was draw coated onto an acrylic sheet using a custom made drawbar with 500 μm gap height. After the film was cured, a stencil was cut out of 25 μm PET film using a UV laser (LPKF Protolaser U4) and placed onto the DS10 films. EGaIn (or bGaIn) was then spread across the mask. Then, copper tape was affixed on each end of the conductive traces using silver epoxy (Part 8331-14G, MGchemicals). Once the silver epoxy cured, square pieces of plain-weave fabric were impregnated with silicone (DS10), placed on each end of the conductive traces, and left to cure for 1 h at 60 °C. The specimens were then encapsulated by draw-coating another layer of silicone (DS10), and left to cure overnight at 60 °C. At this point, the film containing the samples could be lifted and removed from the acrylic sheet. Then, the samples were cut into a dogbone shape using a laser cutter (VLS 3.50, Universal Laser Systems Inc.) at 90% intensity and at 11% speed.

For electromechanical testing, the specimens were subjected to uniaxial tensile loading at 15 mm min^{-1} using a customized tensile stage controlled using an Arduino Uno. The dynamic resistance measurements were acquired using three methods: 1) four point probe, 2) two point probe, and 3) Wheatstone bridge. The resistance and strain values were recorded using Matlab 2021.

Supporting Information

Supporting Information is available from the Wiley Online Library or from the author.

Acknowledgements

Conflict of Interest

The authors declare no conflict of interest.

Keywords

[1] R. Guo, B. Cui, X. Zhao, M. Duan, X. Sun, R. Zhao, L. Sheng, J. Liu, J. Lu, *Mater. Horiz.* **2020**, *7*, 1845.

[2] C. Majidi, R. Kramer, R. J. Wood, *Smart Mater. Struct.* **2011**, *20*.

[3] R. K. Kramer, C. Majidi, R. Sahai, R. J. Wood, *IEEE Int. Conf. Intell. Rob. Syst.* **2011**, pp. 1919.

[4] S. Zhu, J. H. So, R. Mays, S. Desai, W. R. Barnes, B. Pourdeyhimi, M. D. Dickey, *Adv. Funct. Mater.* **2013**, *23*, 2308.

[5] J. W. Boley, E. L. White, G. T. Chiu, R. K. Kramer, *Adv. Funct. Mater.* **2014**, *24*, 3501.

[6] B. A. Gozen, A. Tabatabai, O. B. Ozdoganlar, C. Majidi, *Adv. Mater.* **2014**, *26*, 5211.

[7] S. Y. Tang, J. Zhu, V. Sivan, B. Gol, R. Soffe, W. Zhang, A. Mitchell, K. Khoshmanesh, *Adv. Funct. Mater.* **2015**, *25*, 4445.

[8] A. B. T. Haque, R. Tutika, M. Gao, A. Martinez, J. Mills, J. A. Clement, J. Gao, M. Tabrizi, M. R. Shankar, Q. Pei, M. D. Bartlett, *Multifunct. Mater.* **2020**, *3*, 044001.

[9] T. Jung, S. Yang, *Sensors* **2015**, *15*, 11823.

[10] S. Cheng, Z. Wu, *Adv. Funct. Mater.* **2011**, *21*, 2282.

[11] J. Wissman, M. D. Dickey, C. Majidi, *Adv. Sci.* **2017**, *4*, 1700169.

[12] M. Zadan, M. H. Malakooti, C. Majidi, *ACS Appl. Mater. Interfaces* **2020**, *12*, 17921.

[13] C. Dong, A. Leber, T. D. Gupta, R. Chandran, M. Volpi, Y. Qu, T. Nguyen-Dang, N. Bartolomei, W. Yan, F. Sorin, *Nat. Commun.* **2020**, *11*, 3537.

[14] Y. C. Lai, H. W. Lu, H. M. Wu, D. Zhang, J. Yang, J. Ma, M. Shamsi, V. Vallem, M. D. Dickey, *Adv. Energy Mater.* **2021**, *11*, 2100411.

[15] J. K. Paik, R. K. Kramer, R. J. Wood, in *IEEE Int. Conf. on Intelligent Robots and Systems*, IEEE, Piscataway, NJ **2011** pp. 414–420.

[16] Y. Mengüç, Y. L. Park, H. Pei, D. Vogt, P. M. Aubin, E. Winchell, L. Fluke, L. Stirling, R. J. Wood, C. J. Walsh, *Int. J. Rob. Res.* **2014**, *33*, 1748.

[17] J. Wu, S. Y. Tang, T. Fang, W. Li, X. Li, S. Zhang, *Adv. Mater.* **2018**, *30*, e1805039.

[18] H. Chang, P. Zhang, R. Guo, Y. Cui, Y. Hou, Z. Sun, W. Rao, *ACS Appl. Mater. Interfaces* **2020**, *12*, 14125.

[19] K. B. Ozutemiz, J. Wissman, O. B. Ozdoganlar, C. Majidi, *Adv. Mater. Interfaces* **2018**, *5*, 1701596.

[20] C. Pan, K. Kumar, J. Li, E. J. Markvicka, P. R. Herman, C. Majidi, *Adv. Mater.* **2018**, *30*, 1706937.

[21] R. A. Bilodeau, A. M. Nasab, D. S. Shah, R. Kramer-Bottiglio, *Soft Matter* **2020**, *16*, 5827.

[22] Y. G. Park, H. Min, H. Kim, A. Zhexembekova, C. Y. Lee, J. U. Park, *Nano Lett.* **2019**, *19*, 4866.

[23] S. Park, G. Thangavel, K. Parida, S. Li, P. S. Lee, *Adv. Mater.* **2019**, *31*, 1805536.

[24] L. Cao, D. Yu, Z. Xia, H. Wan, C. Liu, T. Yin, Z. He, *Adv. Mater.* **2020**, *32*, 2000827.

[25] R. Guo, X. Wang, H. Chang, W. Yu, S. Liang, W. Rao, J. Liu, *Adv. Eng. Mater.* **2018**, *20*, 1800054.

[26] U. Daalkhaijav, O. D. Yirmibesoglu, S. Walker, Y. Mengüç, *Adv. Mater. Technol.* **2018**, *3*, 1700351.

[27] S. Liu, D. S. Shah, R. Kramer-Bottiglio, *Nat. Mater.* **2021**, *20*, 851.

[28] Y. Li, S. Feng, S. Cao, J. Zhang, D. Kong, *ACS Appl. Mater. Interfaces* **2020**, *12*, 50852.

[29] P. A. Lopes, D. F. Fernandes, A. F. Silva, D. G. Marques, A. T. D. Almeida, C. Majidi, M. Tavakoli, *ACS Appl. Mater. Interfaces* **2021**, *13*, 14552.

[30] M. Tavakoli, M. H. Malakooti, H. Paisana, Y. Ohm, D. G. Marques, P. A. Lopes, A. P. Piedade, A. T. de Almeida, C. Majidi, *Adv. Mater.* **2018**, *30*, 1801852.

[31] J. Wang, G. Cai, S. Li, D. Gao, J. Xiong, P. S. Lee, *Adv. Mater.* **2018**, *30*, 1706157.

[32] M. H. Malakooti, M. R. Bockstaller, K. Matyjaszewski, C. Majidi, *Nanoscale Adv.* **2020**, *2*, 2668.

[33] S. Chen, H. Z. Wang, R. Q. Zhao, W. Rao, J. Liu, *Matter* **2020**, *2*, 1446.

[34] M. B. Heane, *Electrical Conductivity and Resistivity*, 2nd ed., CRC Press, Boca Raton, FL **2014**, pp. 26–1–26–15.

[35] T. Sato, K. Yamagishi, M. Hashimoto, E. Iwase, *ACS Appl. Mater. Interfaces* **2021**, *13*, 18247.

[36] E. L. White, M. C. Yuen, J. C. Case, R. K. Kramer, *Adv. Mater. Technol.* **2017**, *2*, 1700072.

[37] N. Zolfaghari, P. Khandagale, M. J. Ford, K. Dayal, C. Majidi, *Soft Matter* **2020**, *16*, 8818.

[38] M. D. Dickey, *Adv. Mater.* **2017**, *29*, 1606425.

[39] W. Wu, *Sci. Technol. Adv. Mater.* **2019**, *20*, 187.

[40] S.-H. Sunwoo, K.-H. Ha, S. Lee, N. Lu, D.-H. Kim, *Annu. Rev. Chem. Biomol. Eng.* **2021**, *12*, 359.

[41] Y. L. Park, B. R. Chen, R. J. Wood, *IEEE Sens. J.* **2012**, *12*, 2711.

[42] M. J. Ford, C. P. Ambulo, T. A. Kent, E. J. Markvicka, C. Pan, J. Malen, T. H. Ware, C. Majidi, *Proc. Natl. Acad. Sci. USA* **2019**, *116*, 21438.

[43] E. J. Markvicka, M. D. Bartlett, X. Huang, C. Majidi, *Nat. Mater.* **2018**, *17*, 618.

[44] A. Fassler, C. Majidi, *Adv. Mater.* **2015**, *27*, 1928.

[45] D. Zrnic, D. Swatik, *J. Less-Common Metals* **1969**, *18*, 67.

[46] S. Cheng, Z. Wu, *Lab Chip* **2012**, *12*, 2782.

[47] T. V. Neumann, B. Kara, Y. Sargolzaeiaval, S. Im, J. Ma, J. Yang, M. C. Ozturk, M. D. Dickey, *Micromachines* **2021**, *12*, 1.

[48] Z. Ma, Q. Huang, Q. Xu, Q. Zhuang, X. Zhao, Y. Yang, H. Qiu, Z. Yang, C. Wang, Y. Chai, Z. Zheng, *Nat. Mater.* **2021**, *20*, 859.

[49] J. E. Park, H. S. Kang, M. Koo, C. Park, *Adv. Mater.* **2020**, *32*, 2002178.

[50] E. Porte, R. Kramer-Bottiglio, *Advanced Materials Technologies* **2021**, *6*, 2001247.

**ADVANCED
SCIENCE NEWS**

www.advancedsciencenews.com

**ADVANCED
MATERIALS**

www.advmat.de

Lina Sanchez Botero received her B.S. in Engineering Physics and M.S. in Applied Physics from the National University of Colombia. She completed her Ph.D. degree at Cornell University under the supervision of Professor Juan Hinestroza, in 2018. She is currently a Postdoctoral Associate in Mechanical Engineering and Materials Science at Yale University in Rebecca Kramer-Bottiglio's Lab. Her current research interests include advanced manufacturing and materials development, soft and wearable technologies, and human-machine interaction.

Dylan Shah received his B.S. in mechanical engineering and M.S. in Agricultural Engineering from Iowa State University, in 2015 and 2016, respectively. He completed a Ph.D. degree at Yale University under the supervision of Professor Rebecca Kramer-Bottiglio in 2022 and was a NASA Space Technology Research Fellow in collaboration with Massimo Vespignani at NASA Ames Research Center. His research contributes to the fields of soft robotics, reconfigurable robotics, and stretchable electronics.

Rebecca Kramer-Bottiglio is an associate professor at Yale University. She leads the Faboratory, which innovates in materials, manufacturing, and robotics to develop new multifunctional materials that will allow next-generation robots to adapt their morphology and behavior to changing tasks and environments. Prior to joining Yale, she held a faculty position at Purdue University. She received her B.S. from the Johns Hopkins University, M.S. from UC Berkeley, and Ph.D. from Harvard University.